

The PMC-Amended DB Boundary – A Canonical EBG Surface

Per-Simon Kildal¹, Ahmed Kishk^{1,2}, Marko Bosiljevac³, and Zvonimir Sipus³

¹ Department of Signals and Systems
Chalmers University of Technology, 41296 Gothenburg, SWEDEN
per-simon.kildal@chalmers.se

² Department of Electrical Engineering
University of Mississippi, University, MS 38677-1848, USA
ahmed@olemiss.edu

³ Faculty of Electrical Engineering and Computing
University of Zagreb, HR-10000 Zagreb, Croatia
marko.bosiljevac@fer.hr, zvonimir.sipus@fer.hr

Abstract — Replacing realistic materials and structures by their ideal counterparts, canonical surfaces, is of great interest for initial and conceptual electromagnetic (EM) studies. The recently introduced DB boundary is defined by a set of simple boundary conditions forcing the normal components of the D- and B- fields to be zero at the boundary. We show that this DB boundary produces many 2-D scattering results that are similar to how practical so-called electromagnetic bandgap (EBG) surfaces behave within the bandgap. Still, it is not directly useable as a canonical EBG surface, because, as we demonstrate in this paper, it is incomplete, creating an anomaly for normal incidence which causes unphysical field solution for 3-D field problems. We have removed this anomaly by introducing the PMC-amended DB boundary. This works in the same way as a practically realized EBG surface for both 2-D and 3-D problems within the bandgap, and is therefore a canonical EBG surface.

Index Terms — DB boundary, EBG surfaces, mushroom surface.

I. INTRODUCTION

The present paper will explain some simplified and ideal boundary conditions that can be referred to as canonical surfaces because they

have a physically realizable counterpart. Such canonical surfaces are useful for the further development and unification of the metamaterials area. These ideal boundary conditions include perfect electric conductors (PEC), perfect magnetic conductors (PMC), ideal soft and hard surfaces [1] (represented by PEC/PMC strip grids [2]), and the newly introduced DB boundary [3]. Each of them has a physical realizable counterpart, provided in the latter case that the original DB boundary condition is amended. The present paper will show that the physical counterpart of the amended DB surface is the electromagnetic bandgap (EBG) surface. The name DB boundary refers to the fact that the vertical components of both the D-field and the B-field at the boundary are defined to be zero.

The anisotropic soft surface was introduced in analogy with acoustics to explain why certain surfaces stop waves from propagating along them. Later, it was shown that isotropic high impedance surfaces could stop surface waves as well [4]. The latter are now more correctly referred to as electromagnetic bandgap surfaces, because most so-called high impedance surfaces only have high surface impedance for normal incidence, whereas the wave-stop characteristics are related to the non-existence of surface waves along the surface, and not to this high surface impedance. The hard surface was introduced as the complement to the

original soft surface, allowing waves of any polarization to propagate freely along it. This was then used for removing blockage by cylindrical objects [5], nowadays referred to as cloaking [6].

The guest editorial in [7] gave a joint comprehensive presentation of the EBG surfaces and the soft and hard surfaces by defining ideal canonical surfaces and their boundary conditions, but it also stated the lack of a simple boundary condition for the EBG surface. The present paper explains how the newly introduced DB boundary [3] can be amended to provide such a simple boundary condition and thereby can represent an ideal EBG surface, or in other words an ideal, isotropic and polarization-independent soft surface. The amendment is needed because the DB boundary condition is undefined for normal incidences, i.e., it is incomplete and needs to be amended. As a result, an anomaly appears in some field solutions. The present paper shows how the DB boundary condition can be amended to avoid such anomalies, providing the direction of wave propagation along the EBG surface is known. The amended DB surface is referred as a PMC-amended DB surface.

The computational and analytical simplifications offered by the canonical surfaces have already proven to be advantageous for numerical solutions [8] and generation of conceptually new microwave devices, such as the invisible hard struts in [5] representing the first metamaterial cloak, and the new gap waveguide described in [9]. The latter is a generalization of the single hard-wall parallel-plate waveguide [10], and represents a way to guide local waves (beams) in the gap between parallel metal plates. It originates from the miniaturized hard waveguide in [11-12], and the concept can also be used for packaging of microstrip circuits [13]. The gap waveguides make use of high impedance surface or EBG surface to suppress parallel plate modes, a physical phenomenon that is easily explained in terms of the ideal PMC or amended DB boundaries, respectively.

II. CANONICAL SURFACES: PEC, PMC, PEC/PMC STRIP GRID, PMC-AMENDED DB BOUNDARY

Artificial surfaces like soft and hard surfaces, artificial magnetic conductors, high impedance

surfaces, and electromagnetic bandgap surfaces can be used to control wave propagation: enhance it in desired directions, stop it in undesired directions, and improve polarization characteristics of both. These properties can be explained by reference to Table 1. This was first presented in [2], updated and improved in [6], and it is here extended by introducing the PMC-amended DB boundary as a canonical surface having similar property as the EBG surface at the “best” frequency within the bandgap. The table contains also the related D'B' boundary as explained below. The boundary conditions of the ideal canonical surfaces are also added to Table 1. Notice that we did not impose any frequency dependence of the boundary condition because we consider ideal surfaces. Actual realizations of the canonical surfaces will always have strong frequency dependences (except for the PEC).

The explanations of the boundaries are:

Perfect Electric Conductor (PEC): This surface is widely used in most EM modeling and computations as it describes metal conductors very well when analyzing guiding or radiating properties in the microwave region. The boundary conditions are well defined.

Perfect Magnetic Conductor (PMC): The EM field theory is easily extended to allow PMC. This surface does not exist naturally, but it can be realized artificially within frequency bands and is then referred to as an artificial magnetic conductor (AMC). The ideal boundary condition is well defined and it appears often in practice at the beginning of the frequency band of operation of the AMC.

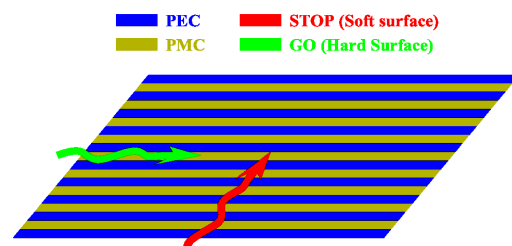


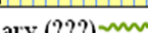
Fig. 1. Visualization of the PEC/PMC strip grid showing the STOP and GO directions.

PEC/PMC strip grid: This is the physical equivalent of an ideal soft/hard surface, see Fig. 1. The surface has locally infinite and unidirectional electric and magnetic conductivity, i.e. both the electric and magnetic currents can only flow in the

strips direction. The PEC/PMC strips can follow any arbitrarily shaped path of planar or non planar form. For the transverse soft case (STOP surface) the PEC/PMC strip grids form electric/magnetic current fences that stop wave propagation, and for the longitudinal hard case (GO surface) they form electric/magnetic current lanes that enhance wave propagation. The ideal boundary conditions are well defined, and many realizations exist. The two most common realizations are corrugations and metal-strip-loaded grounded dielectric substrates. In the first case the ridges of the corrugations represent PEC strips, while the PMC strips are obtained by $\lambda/4$ transformers formed by the

being zero, but we limit our practical interpretations to surfaces in vacuum or air.) Thereby, it stops waves at grazing angles for both horizontal and vertical polarizations for all angles of incidence. Therefore, it works similar to an EBG surface, or in other words like an isotropic soft surface. The boundary condition is well defined, except for the case of a plane wave under vertical (normal) incidence to the surface. For normal plane wave incidence the incoming fields have no vertical components, and therefore the boundary condition is automatically satisfied for any reflection coefficient. Thus, the reflection coefficients as well as the boundary conditions are

Table 1: **Left:** Characteristics of different types of canonical surfaces with respect to propagation of waves along the surface for different E-field polarizations. VER means vertical polarization (i.e. TM-case), HOR means horizontal (i.e. TE-case). The background color and pattern symbolize the PEC (yellow), PMC (blue) and PEC/PMC strips (parallel yellow and blue strips). The different orientations of the colored strips for the soft and hard cases symbolize STOP (current fences) and GO (current lanes) characteristics for waves propagating from left to right (as shown by the arrows) in the paper plane. The colored background in the box of the DB boundary is a PMC-type EBG symbolized by the texture of Sievenpiper's EBG mushroom surface. The D'B' surface has no known realization. **Right:** Ideal boundary conditions of the canonical surfaces. The boundary conditions of the DB and D'B' boundaries are in Lindell's work described in terms of the D and B fields rather than E and H, but here we have chosen the more common E and H field boundary conditions that are equivalent to the original boundary conditions for our practical case considering the interface to an air-filled region.

Canonical Surface	E-field Polarization		
	VER (TM)	HOR (TE)	
PEC	GO	STOP	
PMC	STOP	GO	
PEC/PMC Strip grid	SOFT 	STOP	STOP
	HARD 	GO	GO
PMC-amended DB boundary	EBG 	STOP	STOP
D'B' boundary (???) 	GO	GO	

Ideal boundary condition (in xy-plane)
$E_x = E_y = 0 \ \& \ \partial E_z / \partial z = 0$
$H_x = H_y = 0 \ \& \ \partial H_z / \partial z = 0$
$E_y = 0 \ \& \ H_x = 0$
$E_x = 0 \ \& \ H_x = 0 \ \partial E_z / \partial z = 0$
$E_z = 0 \ \& \ H_z = 0$, amended by (1)
$\partial E_z / \partial z = 0 \ \& \ \partial H_z / \partial z = 0$ (incomplete)

grooves. In the metal-strip-loaded case, the strips naturally represent PEC strips, and the PMC strips are obtained similarly as in the corrugated case by $\lambda/4$ transformers present between the ground plane and the dielectric surface. The ideal boundary conditions appear also for these realizations in the beginning of the frequency band where they work as soft or hard surfaces.

DB boundary: The boundary condition states that both the vertical E and the vertical H field components are zero. (The original formulation is vertical D and the vertical B field components

undefined for normal incidence, or in other words the boundary condition is incomplete. In most cases this will mean that the normally incident waves will pass through the boundary. The reflection coefficient of a realized EBG surface has always a phase that varies with elevation angle for TE case, in such a way that it appears like a PEC for grazing incidence and like a PMC for normal incidence. The anomaly of the reflection properties of the ideal DB boundary for normal incidence has therefore some relation to peculiarities of its practical counterpart. This

anomaly causes some strange unphysical field solutions for some special cases and needs therefore to be corrected. This will be discussed in the next section.

D'B' boundary: By analogy with the DB boundary, the D'B' boundary is an isotropic hard surface defined by the boundary conditions seen in Table 1. However, in contrast to the DB boundary no realization of the D'B' boundary is known so at present it is of little practical interest.

The characteristics of the three different surfaces with respect to polarization of the grazing waves are also illustrated in Table 1. The PEC supports vertically polarized waves that can propagate with strong amplitude; it is a “GO” surface for vertical polarization. These propagating waves are not really surface waves in the mathematical sense, because they are represented by a branch point rather than a pole in the spectral domain. Thus, they are for the ideal case surface waves at cut-off (linked to the corresponding space waves) rather than normal isolated surface waves trapped by the surface. However, when the surface has a thin dielectric coating, the wave along the surface becomes a TM surface wave (i.e. a pole). The PEC STOPS effectively horizontally polarized waves, because the horizontal field component is zero. The PMC behaves naturally in the opposite (dual) way; it is a GO surface easily passing waves along it for horizontal polarization and a “STOP” surface for vertical polarization (see table). The classical soft/hard surfaces can be represented physically by a PEC/PMC strip grid as explained above and illustrated in the table as well. This will STOP waves propagating with both horizontal and vertical polarizations when the strips are oriented transverse to the direction of propagation (soft case), and it will allow the waves to pass (i.e. GO) when they are oriented longitudinally in the same direction as the waves propagate (hard case).

The soft/hard surfaces were originally realized by metal corrugations or metal strips loading a grounded substrate. The soft/hard characteristics appear when they are oriented transversely/longitudinally with respect to the direction of wave propagation. For the soft case, they form so-called electric and magnetic current fences that stop the waves, and for the hard case they form electric and magnetic current lanes that enhance wave propagation.

III. AMENDING THE ORIGINAL DB BOUNDARY

The realized 2-D periodic EBG surfaces behave normally like PMC within some frequency band (or bands) for wave incidence close to normal. However, for wave incidence close to grazing angle and within the lower part of the same frequency band, the EBG surfaces behave more like transverse PEC/PMC strip surface, i.e. like a soft surface stopping waves. The original anisotropic 1-D periodic soft surface has STOP characteristics over an infinite bandwidth for the TE case (i.e. horizontal polarization), provided the period is small enough. Still, the 2-D EBG surfaces are preferable in some applications (such as in the cut-off regions of gap waveguides) because they are isotropic, stopping waves from any direction. For grazing incidence, the 2-D periodic EBG surfaces normally transform from STOP to PMC-type surface at the upper edge of the stop band. These rather complex characteristics of the 2-D EBG surfaces make them impossible to categorize completely in terms of PEC and PMC boundary conditions. However, as stated in the table, the DB boundary characterizes them well. Still, practical EBG surfaces may also be used as PMC ground planes (for low profile electric current radiators), and this characteristic the DB boundary cannot capture. In fact, as already stated before, the DB boundary condition has no effect on normal incident waves, i.e. the solution is undefined which makes the boundary condition incomplete. Therefore, the original DB boundary condition needs to be completed, or amended.

We propose here to amend the original DB boundary condition in the following way:

$$\begin{aligned} \text{Original DB boundary: } E_n &= 0, H_n = 0 \\ \text{Amended DB boundary: } E_n &= 0, H_n + jH_l = 0 \end{aligned} \quad (1)$$

where E_n and H_n are normal components of the E- and H-fields at the boundary and H_l is the longitudinal component in the direction of wave propagation along the surface. Here we prefer to be more general and for that reason we have introduced a local surface normal \mathbf{n} , which is referred to by the index z in Table 1. This means that the amendment only can be used if we know the direction of wave propagation along the

surface. This is not always known, but luckily in most antenna problems the direction of wave propagation is well known.

We will now study field solutions obtained analytically and numerically for two illustrative cases, plane wave scattering from an EBG cylinder and radiation from a horizontal dipole over an EBG surface. The purpose is to visualize the anomaly appearing for the latter case, and to show that the proposed amendment gives results in agreement with numerical simulations which include all the details of the practically realized EBG structure.

IV. SCATTERING FROM CYLINDER WITH EBG SURFACE

In order to understand the characteristics of the DB boundary and confirm our assessments, we first compare its behavior with other canonical surfaces. The series solutions for the scattering from circular cylinders are considered in this section. The scattering from a DB circular cylinder due to the normal plane wave incidence is found to be exactly the same as the scattering from a circular cylinder of PEC/PMC strips directed longitudinally parallel to the cylinder axis [14, 15]. Also, for plane wave under grazing incidence (along the cylinder axis) the scattering from a DB cylinder is exactly the same as for a cylinder with circumferentially directed PEC/PMC strips. However, these exact equalities are only true if the undefined boundary condition is neglected at the point along the cross section of the cylinder where the wave has normal incidence at the DB boundary itself. It is here argued that this point can be neglected because it represents an infinitesimally small part of the complete circumferential boundary. It should also be emphasized that the two series solutions of the PEC/PMC cylinders were obtained by TE/TM decomposition, and that they were verified against 2-D method of moment solutions for TE and TM cases separately. The results are shown in Figure 2. We see that the DB boundary behaves exactly as a soft surface for the two incidences. For normal incidence, the longitudinal PEC/PMC strips define a soft surface, and for grazing incidence, the circumferential strips do.

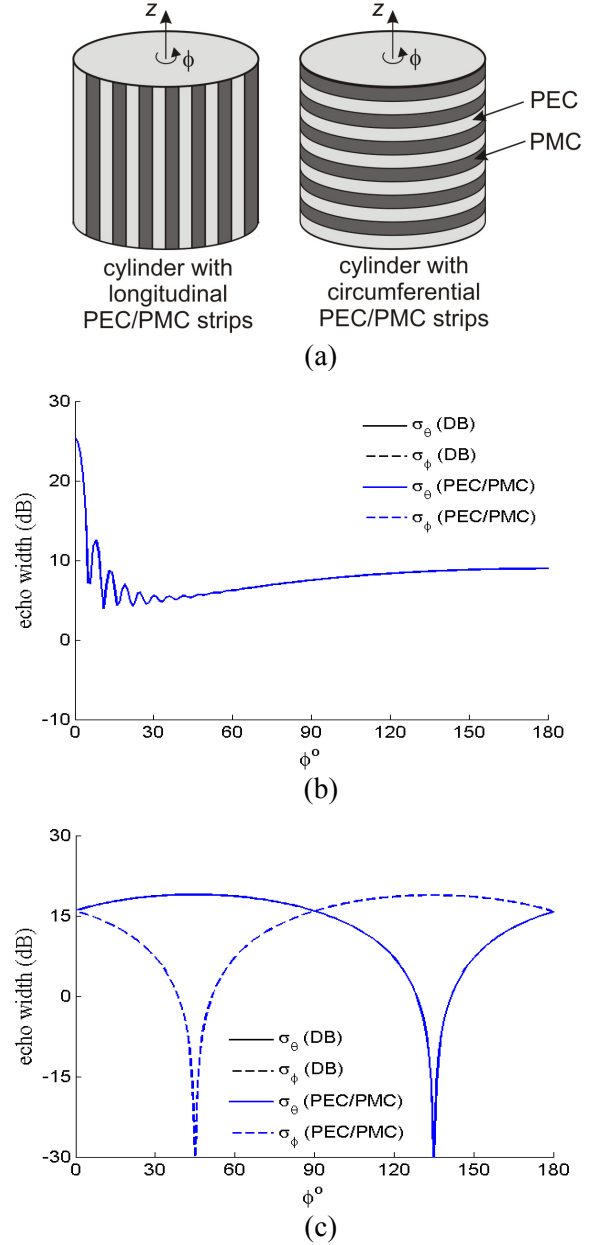
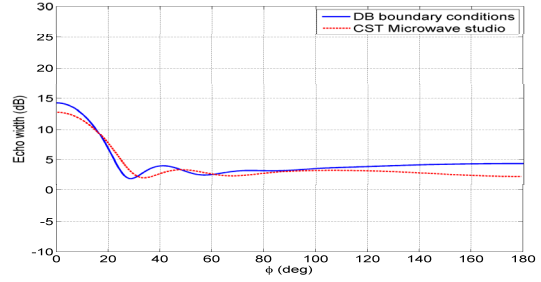
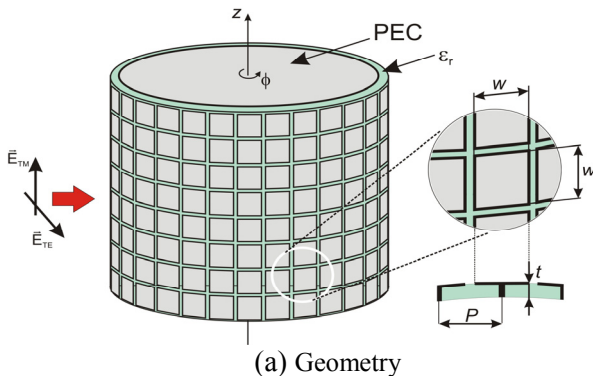


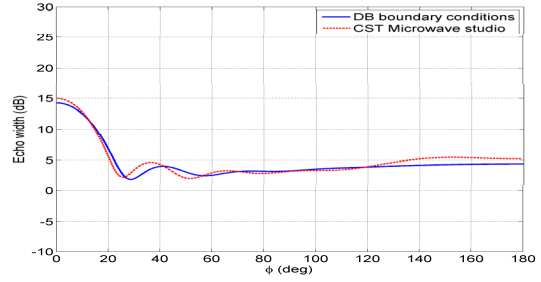
Fig. 2. Echo width of the circular cylinder with geometry shown in (a) for TE and TM cases, i.e. σ_ϕ and σ_θ , respectively. The DB boundary condition is compared with (b) longitudinal PEC/PMC strips forming a circular cylinder due to normal plane wave incidence, and (c) circumferential PEC/PMC strips forming a circular cylinder due to grazing plane wave incidence. Curves not seen explicitly coincide identically with their counterpart. Note that the undefined DB boundary conditions for normal incidence were neglected in these results.

In order to compare the DB boundary conditions to a realistic EBG surface we computed the scattering from a cylindrical mushroom surface by using CST Microwave Studio [15]. The dimensions of the mushroom structure are $w = 2.25$ mm, $P = 2.4$ mm, $t = 1.6$ mm, $\epsilon_r = 2.2$ and the vias diameter is 0.36 mm. The frequency is 12 GHz and the radius of the PEC cylinder is 20 mm. The results are shown in Figs. 3b and c, and we see that there is quite good agreement between the CST results for the practical surface and the series solution for the DB surface.

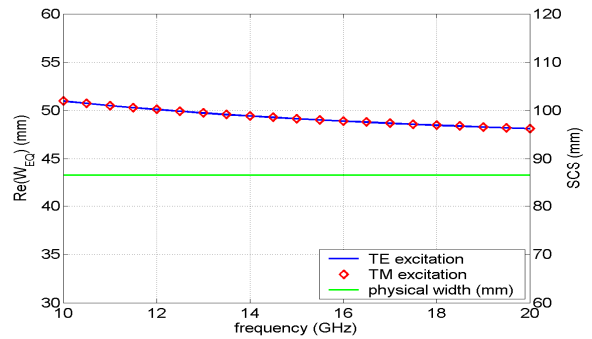
We have also calculated the equivalent blockage width for this DB surface case (Figs. 3d and 3e). The equivalent blockage width (W_{eq}) is a complex-valued parameter (introduced in [5]) that represents the width of an ideal shadow which produces the same forward-scattered field as the cylinder that is being observed (in our case, a DB cylinder). Only the real part of W_{eq} is considered here ($Re(W_{eq})$). The parameter similar to the equivalent blockage width is the scattering cross section per unit length (SCS). It is defined as a ratio of power density of all scattered spatial harmonics and the intensity of the incident Poynting vector. Both the W_{eq} and SCS are the quantities that actually show how wide the cylinder appears for the electromagnetic waves. For lossless scatterers the SCS is equal to $2 \cdot Re(W_{eq})$ according to the forward scattering theorem, being discussed also in [5]. This relation was verified by computation of both SCS and W_{eq} to be satisfied also for cylinders described with DB boundary conditions, therefore there is no leakage of energy present. However, this non-existing leakage problem is in the present case due to the fact that we did not account for the special normal incidence, thereby avoiding that the DB boundary conditions are not defined for normal incidence.



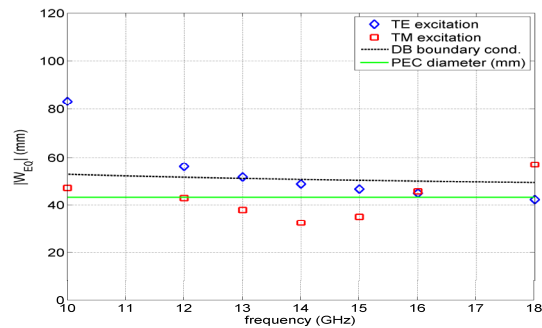
(b) Echo width for TM polarization at 12 GHz



(c) Echo width for TE polarization at 12 GHz



(d) Equivalent blockage width and SCS as a function of frequency for ideal DB cylinder



(e) Equivalent blockage width of ideal DB cylinder and EBG mushroom cylinder (TE and TM polarizations) computed using CST Microwave Studio

Fig. 3. Results for ideal DB cylinder (neglecting normal incidence problem) compared to results for EBG mushroom cylinder obtained by CST Microwave Studio.

V. RADIATION FROM DIPOLE OVER EBG GROUND PLANE

In order to investigate properties of the DB boundary conditions further we consider radiation from a horizontal dipole over a planar EBG surface (see Fig. 4a). Using the plane-wave spectral-domain method in the same way as in [18]-[19], it is easy to determine the Green's functions of the DB boundary, see the Appendix. The G_{xx} component of the dyadic Green's function becomes

$$\tilde{G}_{xx}(z > h) = -\frac{\eta_0 k_x^2 k_z^2 \cos(k_z h) + j \eta_0 k_0^2 k_y^2 \sin(k_z h)}{\beta^2 k_0 k_z} e^{-jk_z z} \tilde{J}_x \quad (2)$$

and equivalently for the other components. From this, the far-field radiation pattern of the horizontal dipole can be determined and is plotted in Fig. 4b.

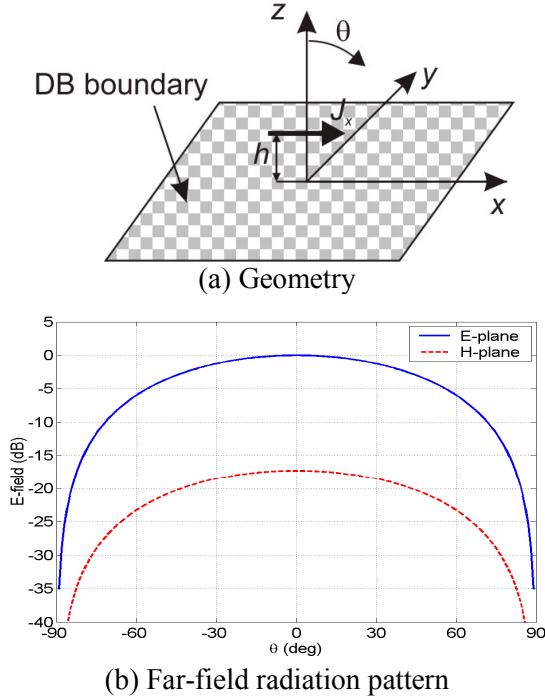


Fig. 4. Horizontal dipole over original DB boundary.

The working frequency is 12 GHz, and the short dipole is located 0.5 mm above the DB boundary. It can be seen that the E-plane and the H-plane do not match at all for $\theta = 0^\circ$, which is wrong as E-plane and H-planes coincide for $\theta = 0^\circ$. This is therefore an anomaly produced by the the DB boundary condition not being defined for $\theta = 0^\circ$. The explanation to the particular results still

achieved is given below. In the E-plane (i.e. for $k_y = 0$), the structure is equal to the x-directed dipole over the transverse (y-directed) PEC/PMC strips [18]. For the specific case $k_y = 0$, corresponding to $\theta = 0^\circ$, we obtain

$$\tilde{G}_{xx}(z > h) = -\frac{\eta_0 k_z \cos(k_z h)}{k_0} e^{-jk_z z} \tilde{J}_x \quad \text{for } k_y = 0 \quad (3)$$

The same Green's functions are obtained in [18] where the Green's functions of a dipole over the PEC/PMC strips surface are derived. However, in the H-plane ($k_x = 0$) we have the x-directed source over the x-directed PEC/PMC strips, which is the same situation as the horizontal dipole over the PEC plane (since the x-component of H-field is zero, the H-field “does not see” the PMC strips). The corresponding Green's function is simply

$$\tilde{G}_{xx}(z > h) = -\frac{j \eta_0 k_0 \sin(k_z h)}{k_z} e^{-jk_z z} \tilde{J}_x \quad \text{for } k_x = 0 \quad (4)$$

We readily see that these two values are not equal for $\theta = 0^\circ$, i.e. when $k_z = k$, thus the anomalous behavior appears.

A. The amended DB boundary

The EM waves that are excited by the horizontal dipole can be represented as a sum of TM and TE plane waves. The problem with the TE waves is that they “feel” that the EBG surface acts as a PEC structure, which is not correct for angles close to normal incidence. We will now first use a more general form of the amended DB boundary condition than that in (1), i.e.

$$H_n + \alpha \cdot H_l = 0, \quad (5)$$

where H_n and H_l denote the normal and the longitudinal component of the magnetic field, respectively, and α is a coefficient (still to be determined). Since the direction of propagation can be determined from k_x and k_y spectral variables, the normal and longitudinal components of the magnetic field are simply

$$H_n = H_z, \quad H_l = \frac{k_x}{\beta} H_x + \frac{k_y}{\beta} H_y. \quad (6)$$

Only the TE polarized wave is of interest (reflection of TM waves is described with the boundary condition $E_z = 0$). Without losing generality let us assume that the wave is propagating in the y -direction, and that θ is the angle of incidence (θ is angle towards z -axis). Therefore, we can write

$$\begin{aligned} k_x &= 0, \\ k_y &= k_0 \cdot \sin \theta, \\ k_z &= k_0 \cdot \cos \theta. \end{aligned} \quad (7)$$

The TE wave can be described with (R is the reflection coefficient)

$$H_z = e^{jk_z z} + R \cdot e^{-jk_z z}, \quad (8)$$

and consequently at $z = 0$ we can now write $H_z = 1 + R$. The y -component of the H -field is equal to

$$H_y = -\frac{jk_y}{\beta^2} \frac{\partial}{\partial z} H_z = -\frac{j}{k_y} \frac{\partial}{\partial z} H_z, \quad (9a)$$

$$H_y = \frac{k_z}{k_y} (e^{jk_z z} - R \cdot e^{-jk_z z}), \quad (9b)$$

and again at $z = 0$ we obtain $H_y = (k_z/k_y)(1 - R)$. The modified DB boundary condition is now equal:

$$(1 + R) + \alpha \cdot \frac{k_z}{k_y} \cdot (1 - R) = 0. \quad (10)$$

Therefore, the reflection coefficient is equal:

$$R = -\frac{1 + \alpha \cdot k_z/k_y}{1 - \alpha \cdot k_z/k_y}. \quad (11)$$

Since we are considering reflection from a surface, we expect $|R| = 1$. Therefore, the only way that $|R| = 1$ for all incidence angles is that α is purely imaginary number. We will simply define coefficient α as $\alpha = -j$. Note that the value of the reflection coefficient is now $R = +1$ for $\theta = 0^\circ$ (PMC for normal incidence) and $R = -1$ for $\theta = 90^\circ$ (PEC for grazing incidence, i.e. soft surface for grazing incidence). We have already in (1) referred

to this special choice of $\alpha = -j$ as the PMC-amended DB boundary condition.

The far-field radiation pattern of a horizontal dipole over a surface described with the corrected DB boundary conditions is given in Fig. 5. Like in the previous case, the working frequency is 12 GHz, and the short dipole is located 0.5 mm above the DB boundary. It can be seen that there now is no problem with singularity at $\theta = 0^\circ$, i.e. the E-plane and the H-plane now match each other at $\theta = 0^\circ$. Furthermore, the radiation pattern reveals that the surface acts as a PMC for angles around normal incidence and that it stops propagating waves for angles close to grazing incidence.

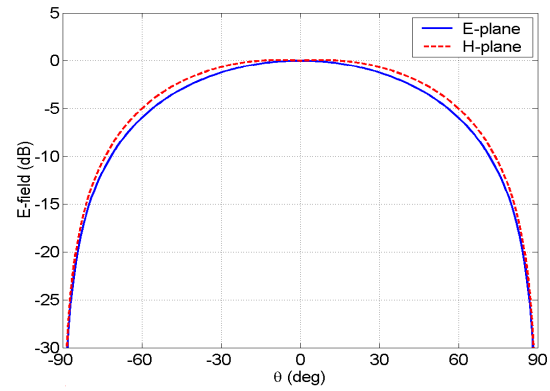
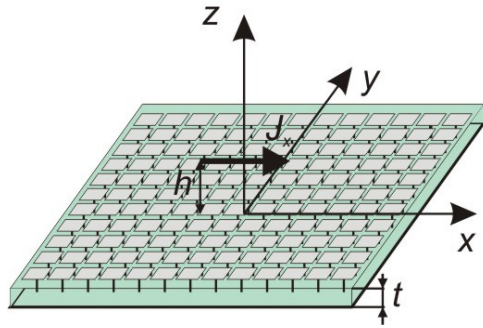


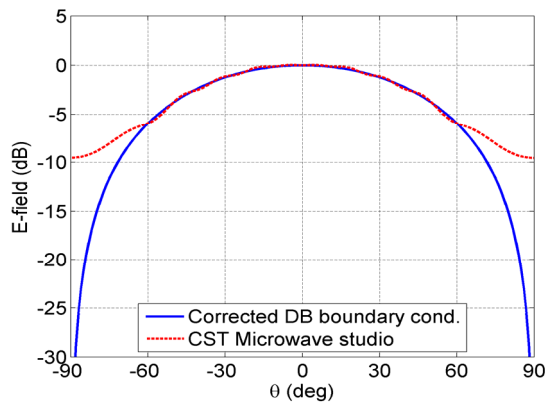
Fig. 5. Far-field radiation pattern of a horizontal dipole over a surface described with PMC-amended DB boundary conditions.

Figure 6 shows comparison of the radiation pattern of the short dipole over the EBG surface realized by the same mushroom structure as in the previous case in Section IV. The working frequency is 12 GHz, i.e. the considered frequency is in the beginning of the stop band which is between 11 and 15 GHz. It can be seen that there is a good agreement between the results for the mushroom structure (modeled with the CST Microwave Studio) and for the canonical EBG surface (modeled with the PMC-amended DB boundary condition) at the best frequency of 12 GHz in the beginning of the bandgap. The frequency dependences of the radiation patterns calculated with both, amended DB boundary conditions and CST, which clearly show that the matching is the best at 12GHz, are shown in Fig. 7. One should note that the considered structures when performing CST calculations were finite and therefore small ripples can be seen due to internal

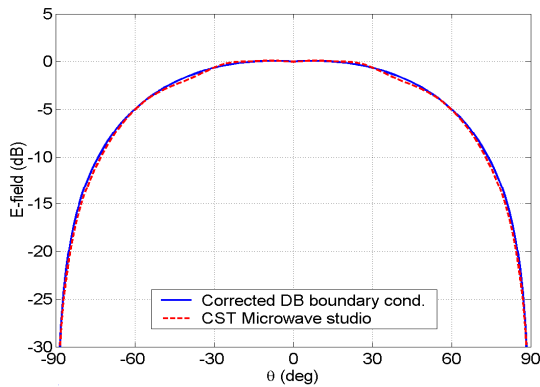
reflection and diffraction from the edges of the structure.



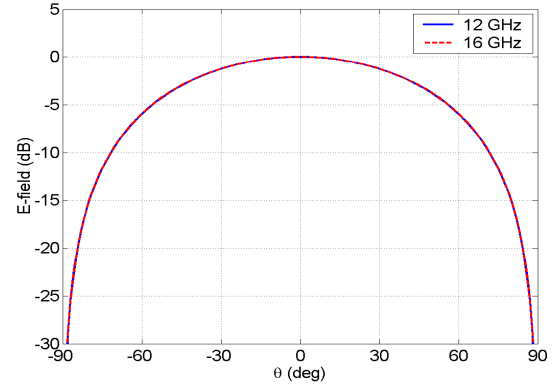
(a) Geometry



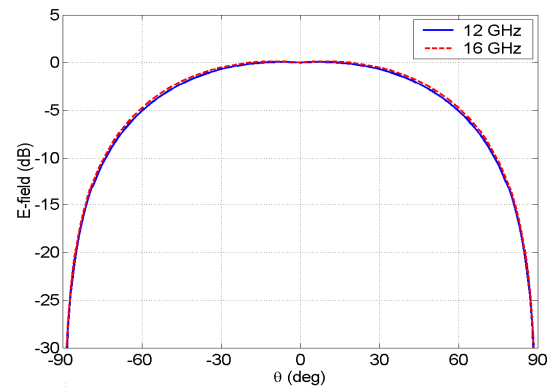
(b) E-plane



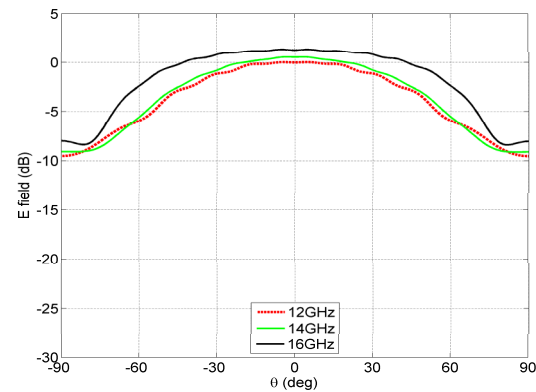
(c) H-plane



(a) E-plane calculated with PMC-amended DB boundary conditions.

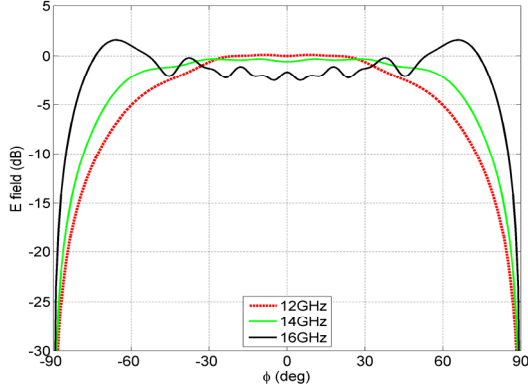


(b) H-plane calculated with PMC-amended DB boundary conditions.



(c) E-plane calculated with CST Microwave Studio.

Fig. 6. Far-field radiation pattern of a horizontal dipole over the PMC-amended DB and EBG surfaces at 12 GHz.



(d) H-plane calculated with CST Microwave Studio.

Fig. 7. Frequency dependence of the far field radiation pattern for the case of a dipole over planar EBG surface.

VI. RADIATION FROM A DIPOLE OVER A CYLINDRICAL PERIODIC STRUCTURE

We would also like to determine how the curvature of the surface influences both the original DB and the PMC-amended DB boundary conditions. In order to do that, we have investigated the radiation of an axially oriented dipole over the cylindrical EBG surface. The problem is described in the classical cylindrical coordinate system: the dipole is z -directed and the surface is described with its radius (we have considered the structure with radius $r_{DB} = 21.6$ mm). The working frequency is 12 GHz and the dipole height over the DB boundary is 0.5 mm. The problem is analyzed using the spectral-domain approach, similarly to the planar case (the details can be found in [19]). The obtained radiation pattern is shown in Fig. 8. It can be seen that there is no problem with singularities for the direction normal to the structure ($\theta = 90^\circ$ and $\phi = 0^\circ$ for the considered structure), i.e. both E-plane and H-plane patterns match in that direction. However, the radiation pattern is not the one we would expect from a dipole over an EBG surface. In more details, the PEC component of the DB boundary prevails over the PMC component, i.e. for the direction normal to the structure the structure acts more like a PEC.

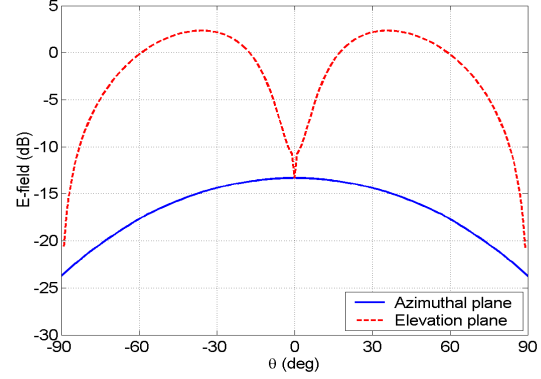
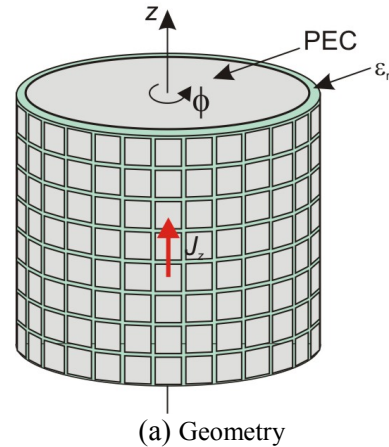
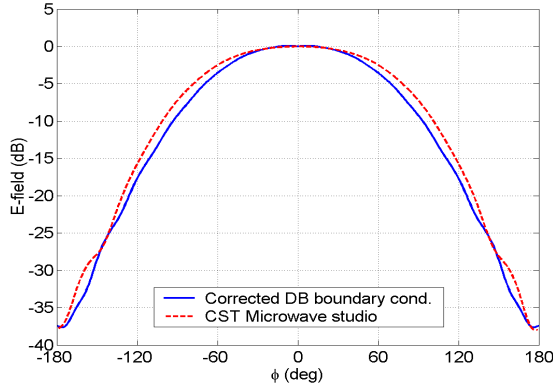


Fig. 8. Far-field radiation pattern of an axially-directed dipole over the cylindrical original DB boundary.

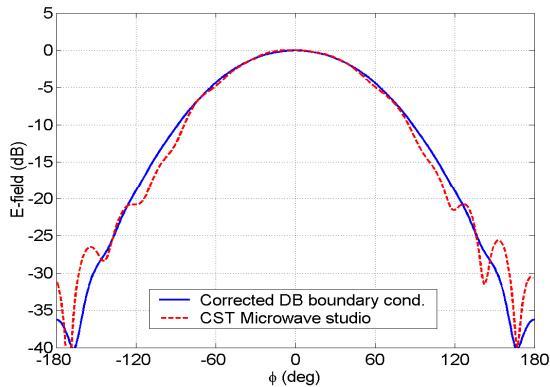
If we apply the PMC-amended DB boundary conditions (defined with the equation (1)), the situation is quite different. In order to compare the DB boundary with a realistic EBG surface we have used the same EBG structure like in the previous case; the working frequency is again 12 GHz. In Fig. 9 we have compared the radiation patterns obtained with corrected DB boundary conditions and with the CST Microwave Studio. It can be seen that the agreement is very good, i.e. the PMC-amended DB boundary condition works very well in describing the main and desired characteristics of the EBG surface. Naturally this is only valid inside the frequency band where the considered structure has a bandgap property. This is clearly seen by viewing Fig. 10 which shows the frequency dependence of this structure, calculated using CST Microwave Studio.



(a) Geometry



(b) Axially-directed dipole



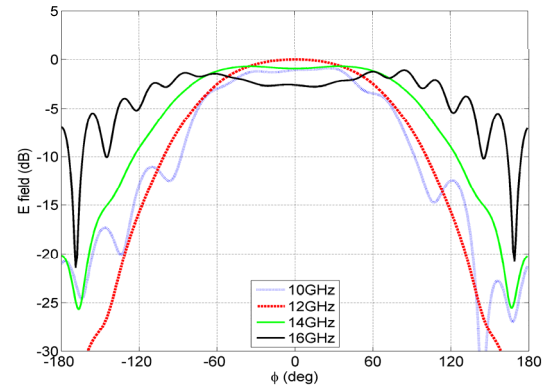
(c) Circumferentially-directed dipole

Fig. 9. Far-field radiation pattern in the azimuth plane of a dipole over the cylindrical PMC-amended DB with EBG surfaces at 12 GHz.

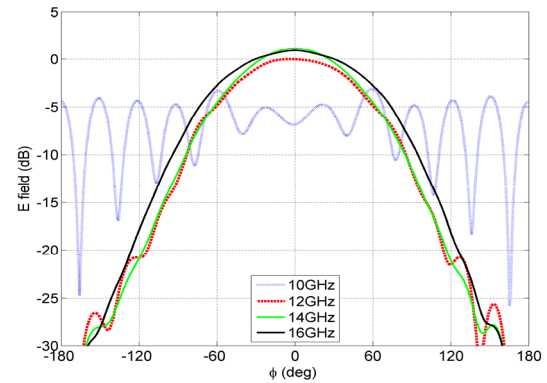
VII. CONCLUSIONS

The paper has summarized previously defined canonical surfaces for use in electromagnetic computations and conceptual studies. The PEC is well accepted and quite extensively used. A similar situation exists for the PMC case, at least in theoretical work and as symmetry planes in EM computations. However, in most computational codes the PMC cannot be used for finite and arbitrary shapes and it cannot be curved. The authors hope that this overview can stimulate software vendors and developers to include arbitrarily shaped PMCs in their codes. This is easily done and will add important capabilities. Similarly, it would be useful if arbitrarily shaped PEC/PMC strip grids with arbitrary strip orientations could be included for general usage. The PEC/PMC strip grids represent soft and hard surfaces and can open up for more fundamental studies and principally new hardware solutions.

The PEC/PMC strip grid is also easy to implement as illustrated in [8].



(a) Axial dipole case



(b) Circumferential dipole case

Fig. 10. Frequency dependence of the far field radiation pattern for the case of a dipole over cylindrical mushroom EBG surface (calculated using CST Microwave Studio).

The newly introduced DB boundary has characteristics similar to an ideal EBG surface, i.e. an isotropic soft surface, but the present paper has highlighted some anomalies that need to be resolved by more research before they can be used in general codes. For a new canonical surface to be meaningful we must require that it is simple and general, and has interesting and useful characteristics. We have proposed a simple amendment in equation (1), referred to as the PMC-amended DB boundary, that seems to work, but it is limited in the sense that it requires knowledge of the propagation direction of the waves along the surface. This limitation is not severe when applied in analytical and semi-analytical modeling like in the present paper. However, for use in general 3-D Moment Method,

FDTD and FEM based field solvers a more general amendment is needed.

There is also the previously introduced so-called D'B' boundary, but this has no known practical counterpart and therefore there is no particular interest for this surface at the moment. The D'B' boundary suffers from a similar anomaly as the DB boundary and also needs to be corrected.

ACKNOWLEDGMENT

The authors are thankful for fruitful discussions with Stefano Maci, Ismo Lindell, and Ari Sihvola.

APPENDIX

The sketch of the structure is given in Fig. 3. The normal EM field component has a form:

$$\begin{aligned}\tilde{E}_z &= A e^{-jk_z(z-d)} \\ H_z &= B e^{-jk_z(z-d)}\end{aligned}\quad \text{for } z \geq d \quad (\text{A1a})$$

$$\begin{aligned}\tilde{E}_z &= C \cos(k_z z) + D \sin(k_z z) \\ \tilde{H}_z &= E \cos(k_z z) + F \sin(k_z z)\end{aligned}\quad \text{for } 0 \leq z \leq d \quad (\text{A1b})$$

The transverse components can be calculated as:

$$\tilde{E}_x = -\frac{jk_x}{\beta^2} \frac{\partial \tilde{E}_z}{\partial z} - \frac{\eta_0 k_0 k_y}{\beta^2} \tilde{H}_z \quad (\text{A2a})$$

$$\tilde{E}_y = -\frac{jk_y}{\beta^2} \frac{\partial \tilde{E}_z}{\partial z} + \frac{\eta_0 k_0 k_x}{\beta^2} \tilde{H}_z \quad (\text{A2b})$$

$$\tilde{H}_x = -\frac{jk_x}{\beta^2} \frac{\partial \tilde{H}_z}{\partial z} + \frac{k_0 k_y}{\eta_0 \beta^2} \tilde{E}_z \quad (\text{A2c})$$

$$\tilde{H}_y = -\frac{jk_y}{\beta^2} \frac{\partial \tilde{H}_z}{\partial z} - \frac{k_0 k_x}{\eta_0 \beta^2} \tilde{E}_z \quad (\text{A2d})$$

$$\beta^2 = k_x^2 + k_y^2. \quad (\text{A2e})$$

The DB boundary conditions at $z = 0$ straightforwardly define two out of six unknowns:

$$E_z = H_z = 0 \quad (\text{A3a})$$

$$\Rightarrow C = E = 0. \quad (\text{A3b})$$

The remaining four boundary conditions are:

$$\begin{aligned}\tilde{E}_x^+ - \tilde{E}_x^- &= 0 \\ \tilde{E}_y^+ - \tilde{E}_y^- &= 0 \\ \tilde{H}_x^+ - \tilde{H}_x^- &= 0 \\ \tilde{H}_y^+ - \tilde{H}_y^- &= -\tilde{J}_x\end{aligned}\quad \text{at } z = h. \quad (\text{A4})$$

The four equations with four unknowns are ‘‘easily’’ analytically solved giving the following results:

$$\begin{aligned}A &= \frac{\eta_0}{k_0} k_x \cos(k_z h) \tilde{J}_x \\ B &= j \frac{k_y}{k_z} \sin(k_z h) \tilde{J}_x \\ D &= -j \frac{\eta_0}{k_0} k_x e^{-jk_z h} \tilde{J}_x \\ F &= j \frac{k_y}{k_z} e^{-jk_z h} \tilde{J}_x.\end{aligned}\quad (\text{A5})$$

From here it is easy to derive all EM field components using equations (A1) and (A2). For example, the E_x component is equal to

$$\tilde{G}_{xx}(z > h) = -\frac{\eta_0 k_x^2 k_z^2 \cos(k_z h) + j \eta_0 k_0^2 k_y^2 \sin(k_z h)}{\beta^2 k_0 k_z} e^{-jk_z z} \tilde{J}_x. \quad (\text{A6})$$

REFERENCES

- [1] P.-S. Kildal, ‘‘Artificially Soft and Hard Surfaces in Electromagnetics,’’ *IEEE Trans. Antennas Propagat.*, vol. 38, pp. 1537-1544, Oct. 1990.
- [2] P.-S. Kildal and A. Kishk, ‘‘EM Modeling of Surfaces with STOP or GO Characteristics - Artificial Magnetic Conductors and Soft and Hard Surfaces,’’ *Applied Computational Electromagnetics Society Journal*, vol. 18, pp. 32-40, Mar. 2003.
- [3] V. Lindell and A. H. Sihvola, ‘‘Electromagnetic Boundary and its Realization with Anisotropic Metamaterial,’’ *Physical Review E* 79, 026604, 2009.
- [4] D. Sievenpiper, L. J. Zhang, R. F. J. Broas, N. G. Alexopolous, and E. Yablonovitch, ‘‘High-Impedance Electromagnetic Surfaces with a

- Forbidden Frequency Band,” *IEEE Transactions on Microwave Theory and Techniques*, vol. 47, pp. 2059-2074, Nov. 1999.
- [5] P.-S. Kildal, A. Kishk, and A. Tengs, “Reduction of Forward Scattering from Cylindrical Objects using Hard Surfaces,” *IEEE Trans. Antennas Propagat.*, vol. 44, pp. 1509-1520, Nov. 1996.
- [6] P.-S. Kildal, A. Kishk, and Z. Sipus, “RF Invisibility using Metamaterials: Harry Potter's Cloak or the Emperor's New Clothes?,” *2007 IEEE International Symposium on Antennas and Propagation (APS)*, Hawaii, 10-15 June 2007.
- [7] P.-S. Kildal, A. A. Kishk, and S. Maci, “Special Issue on Artificial Magnetic Conductors, Soft/Hard Surfaces, and Other Complex Surfaces” (Guest Editors), *IEEE Transactions on Antennas and Propagation*, vol. 53, pp. 2-7, Jan. 2005.
- [8] Ahmed Kishk and Per-Simon Kildal, “Modeling of Soft and Hard Surfaces using Ideal PEC/PMC Strip Grids,” *IET Microwaves, Antennas & Propagation*, vol. 3, pp. 296-302, Mar. 2009.
- [9] P.-S. Kildal, E. Alfonso, A. Valero-Nogueira, and E. Rajo-Iglesias, “Local Metamaterial-Based Waveguides in Gaps between Parallel Metal Plates,” *IEEE Antennas and Wireless Propagation Letters (AWPL)*, vol. 8, pp. 84-87, 2009.
- [10] A. Valero-Nogueira, E. Alfonso, J. I. Herranz, and P.-S. Kildal, “Experimental Demonstration of Local Quasi-TEM Gap Modes in Single-Hard-Wall Waveguides,” *IEEE Microwave and Wireless Components Letters*, vol. 19, pp. 536-538, Sept. 2009.
- [11] M. Ng Mou Kehn and P.-S. Kildal, “Miniaturized Rectangular Hard Waveguides for use in Multi-Frequency Phased Arrays,” *IEEE Transactions on Antennas and Propagation*, vol. 53, pp. 100-109, Jan. 2005.
- [12] M. Ng Mou Kehn, M. Nannetti, A. Cucini, S. Maci, and P.-S. Kildal “Analysis of Dispersion in Dipole-FSS Loaded Hard Rectangular Waveguide,” *IEEE Transactions on Antennas and Propagation*, vol. 54, pp. 2275-2282, Aug. 2006.
- [13] E. Rajo-Iglesias, A. Uz Zaman, and P.-S. Kildal, “Parallel Plate Cavity Mode Suppression in Microstrip Circuit Packages using a Lid of Nails,” *IEEE Microwave and Wireless Components Letters*, vol. 20, no. 1, pp. 31-33, Jan. 2010.
- [14] M. A. Kishk, A. A. Kishk, and P.-S. Kildal, “Electromagnetic Scattering from Circular Cylinders with PEC/PMC Boundaries,” *2010 IEEE International Symposium on Antennas and Propagation*, Toronto, July 11-17, 2010.
- [15] P.-S. Kildal, A. A. Kishk, and Z. Sipus, “Introduction to Canonical Surfaces in Electromagnetic Computations: PEC, PMC, PEC/PMC Strip Grid, DB Surface,” *The 26th Annual Review of Progress in Applied Computational Electromagnetics*. Tampere, Finland, pp. 514-519, April 26-29, 2010.
- [16] CST Microwave Studio 2010, www.cst.com.
- [17] I. V. Lindell, and A. H. Sihvola, “Uniaxial IB-Medium Interface and Novel Boundary Conditions,” *IEEE Transactions on Antennas and Propagation*, vol. 57, pp. 694-700, Mar. 2009.
- [18] Z. Sipus, H. Merkel, and P.-S. Kildal, “Green's Functions for Planar Soft and Hard Surfaces Derived by Asymptotic Boundary Conditions,” *IEE Proceedings - Microwaves, Antennas and Propagation*, vol. 144, pp. 321-328, Oct. 1997.
- [19] Z. Sipus, P.-S. Kildal, R. Leijon, and M. Johansson, “An Algorithm for Calculating Green's Functions of Planar, Circular Cylindrical and Spherical Multilayer Substrates,” *Applied Computational Electromagnetics Society Journal*, vol. 13, no. 3, pp. 243-254, 1998.